06,13,04

X-ray Flashes and Pulsating Electron Flow in X-Ray Generators Based on SBN-61 Crystals

© V.A. Andrianov[1], A.L. Erzinkian[1], L.I. Ivleva[2], P.A. Lykov[2]

[1] Skobeltsyn Institute of Nuclear Physics, Moscow State University, Moscow, Russia
[2] Prokhorov Institute of General Physics, Russian Academy of Sciences, Moscow, Russia

E-mail: andrva22@mail.ru

Received May 23, 2022
Revised May 23, 2022
Accepted May 30, 2022

In an X-ray generator based on a ferroelectric crystal of barium-strontium niobate $Sr_{0.61}Ba_{0.39}Nb_2O_6$ (SBN-61) at a temperature of about 50°C, pulsations of the electron flux and X-ray radiation were detected with an increase in gas pressure in the range $2 \cdot 10^{-2}-10^{-1}$ Torr. The electron flux had the shape of a cross in the crystal plane. The flash duration did not exceed 0.04 seconds. The pulsation period varied from 0.2 seconds at the beginning and up to 5−10 s at the end at a pressure of ≈ 0.1 Torr. The observed effect is explained by the movement of domain boundaries on the depolarized crystal face in vacuum conditions, resulting in a large surface charge and, accordingly, an electric potential, leading to the formation of a pulsed electron flux.

Keywords: X-ray radiation, electron flux, SBN-61 crystal, ferroelectric domains.

DOI: 10.21883/PSS.2022.10.54238.385

1. Introduction

In recent years, the properties of pyroelectric crystals have attracted increased attention in connection with the creation of portable sources of X-ray and neutron radiation. A number of crystals and ceramic samples with large values of the pyroelectric coefficient γ was investigated [1–3]. It has been shown that $LiNbO_3$ and $LiTaO_3$ crystals, $\gamma = 8.3\,\mathrm{nC \cdot cm^{-2}\,K^{-1}}$ and $\gamma = 12\,\mathrm{nC \cdot cm^{-2}\,K^{-1}}$ have the best properties. On the basis of these crystals, commercial products were created [4].

The principle of operation of the pyroelectric X-ray source is as follows (Fig. 1). The pyroelectric crystal *1* is placed in a vacuum chamber *4* on a heater *3*. The axis of spontaneous electrical polarization is directed vertically. Above the crystal is a target *6*. The target has electrical contact with the bottom face of the crystal and the chamber body. On the polar faces of the crystal there are large bound charges Q_{bond}, which are due to the dipole moment of the crystal cell.

Under standard conditions, the charges Q_{bond} are compensated by external charges Q_{comp}, and the total charge is zero: $Q_{\mathrm{sum}} = Q_{\mathrm{bond}} + Q_{\mathrm{comp}} = 0$. When the crystal is heated in a vacuum, the bound charge Q_{bond} decreases, and the compensating charge remains almost constant. As a result, a large uncompensated charge is formed on the outer face of the crystal, creating an electric field. The resulting voltage between the upper face of the crystal and the target U_{gap} can reach large values up to 100 kV. The electric field causes the electrons to be injected and accelerated towards the target. When electrons collide with a target, bremsstrahlung and characteristic X-ray radiation are produced, as in the case of an X-ray tube.

Typically, heating and cooling of crystals are carried out in a cyclic mode, in a vacuum, at about the same speed [1,2]. After the transition from heating to cooling mode, the charge sign at the outer face and, accordingly, the direction of the electron flow change. In this case, the generation of X-ray radiation is preserved, but occurs when the electron beam collides with the crystal.

Currently, work continues on the research of new materials for pyroelectric generators, which could provide better performance properties. In particular, materials that can create high electrical voltages at the level of 100 kV are relevant, capable of supporting the nuclear fusion reactions of type D + D and providing stable generation of neutron radiation [2].

In [5] we investigated crystals of solid solutions of barium-strontium niobate $Sr_{0.61}Ba_{0.39}Nb_2O_6$ (SBN-61), which have a very high pyroelectric coefficient $\gamma = 85\,\mathrm{nC \cdot cm^{-2}K^{-1}}$ [6,7]. The properties of SBN crystals differ from the classical ones: these crystals belong to the class of ferroelectric relaxers, have a diffuse phase transition with a low Curie temperature, about 80°C, and a small electric coercive field [8,9]. In [5] the electron flow and generation of X-ray radiation in SBN crystals were recorded in heating mode. The maximum energy of electron beam determined from the bremsstrahlung boundary was 50 keV at a temperature change of $\Delta T \approx 40$°C.

Not high enough voltage between the upper face of the crystal and the target U_{gap} was explained by the well-known formula [10,11]:

$$U_{gap} = \frac{\gamma(T)\Delta T}{\varepsilon_0} \frac{d_{gap}}{1 + \frac{d_{gap}}{d_{cr}} \varepsilon_{cr}} \approx \frac{\gamma(T)\Delta T}{\varepsilon_0 \varepsilon_{cr}} d_{cr}, \qquad (1)$$

where T — temperature, ΔT — temperature change, γ — pyroelectric coefficient, ε_0 — the absolute permittivity, ε_{cr} — permittivity of the crystal, d_{gap} — the distance between the target and the crystal, d_{cr} — the thickness of the crystal.

The voltage U_{gap} determines the energy of the electron beam and, accordingly, the maximum energy of the X-ray radiation. As it follows from the formula (1) that when comparing different materials, the main parameter is the ratio of $F_1 = \gamma(T)/\varepsilon_{cr}$. For $LiNbO_3$ the permittivity is $\varepsilon_{cr} = 30$, and the F_1 parameter is 0.28. Accordingly, if the thickness of the crystal $d_{cr} = 10$ mm and $\Delta T = 40°C$, the voltage is expected to be $U_{gap} \approx 100$ kV. The SBN crystal is characterized by a large permittivity $\varepsilon_{cr} = 800$ [6,7], and the parameter F_1 is 0.11, i.e. the generated voltage will be about 2.5 times less than in the case of $LiNbO_3$.

X-ray generation in SBN crystals was observed only in heating mode. When cooling crystals in a vacuum, X-ray radiation was absent, and a number of unusual effects were observed, the description of which was devoted to this work.

2. Experiment

In this work the crystals $Sr_{0.61}Ba_{0.39}Nb_2O_6$ (SBN-61), grown by Stepanov's modified method at the Institute of General Physics of the Russian Academy of Sciences (Moscow, Russia) [12] were used. The samples studied had the form of transparent parallelepipeds cut along the crystallographic axes *a, b* and with dimensions of approximately $14 \times 9.3 \times 13$ mm, respectively. Samples were polarized along the polar axis c in an electric field 6 kV/cm at room temperature for several hours, followed by measurement of the half-wave voltage by the dynamic method [13]. The degree of completeness of polarization was controlled by comparing the obtained values of half-wave voltage with the values characteristic of crystals of this composition. Electrical contacts were made by conductive glue based on colloidal carbon.

The experiments were carried out in the vacuum chamber, the scheme of which is shown in Fig. 1. The crystal *1* was attached to a copper plate *2* mounted on a thermoelectric Peltier module *3*. The upper face of the crystal had a positive polarity (the $c+$ face). The Peltier module provided heating and cooling of the crystal. The temperature was measured with a chromel-alumel thermocouple *5* fixed on a plate *2* next to the crystal. The bottom face of the crystal $(c-)$ together with the plate *2* was grounded to the metal body of the chamber *4*. Above the crystal at a distance of about 7 mm there was a target *6*,

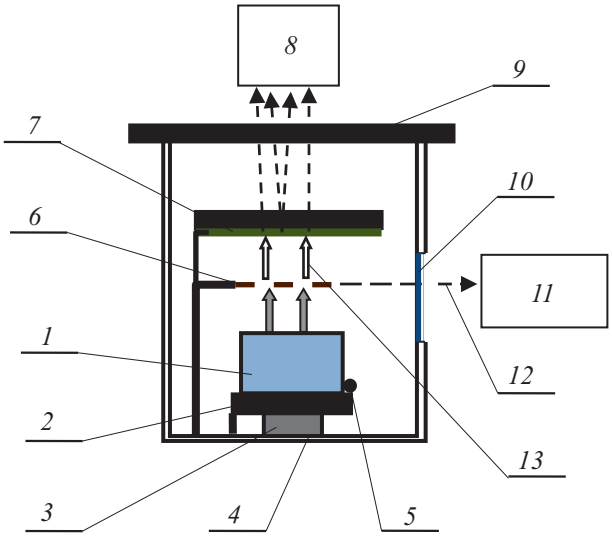

Figure 1. The scheme of the working chamber. *1* — pyroelectric crystal, *2* — copper plate, *3* — heater (Peltier module), *4* — chamber housing, *5* — thermometer (thermocouple), *6* — mesh target, *7* — phosphor, *8* — photo/video equipment, *9* — glass window, *10* — beryllium window, *11* — photoelectronic multiplier, *12* — X-ray radiation, *13* — electron flow.

which in our case was a tungsten grid with a pitch of 2×2.5 mm. The grid *6* was also grounded on the camera body. The fluorescent screen *7* was placed above the grid *6* at a distance of about 7 mm. The glow of the fluorescent screen caused by the electron beam *13* emerging from the crystal was recorded by digital photo and video equipment *8* through a glass window *9*. The beryllium window *10* for X-ray radiation *12* was located on the side of the chamber. X-ray radiation was recorded by a photomultiplier *11* with a thin NaI(Tl) crystal having an energy resolution of 3.2 keV on the line 5.9 keV.

The experiment was carried out in a vacuum $\approx 10^{-3}$ Torr. The crystal was heated by a Peltier module to a temperature of about 60°C at a rate of 0.05 K/s, then kept at a maximum temperature of 10 min to ensure a transition to an equilibrium state. Cooling of the crystal was carried out at a speed of 0.05 K/s to a temperature of $\approx 10°C$. Before reheating, the crystal was also kept for 10 min at a temperature of 10 K.

The experiment recorded X-ray radiation (characteristic and bremsstrahlung), which occurred when an electron beam collided with the target (tungsten grid). The spatial structure of the electron flow passing through the grid target was visualized on the phosphor and recorded by photo and video equipment.

As indicated in the Introduction, electron flow and X-ray radiation was observed when heated in a vacuum, there was no radiation when cooled in a vacuum [5]. This behavior differs from the properties of traditional crystals $LiNbO_3$ and $LiTaO_3$, in which the direction of the electron flow changes upon cooling, but X-ray generation of is

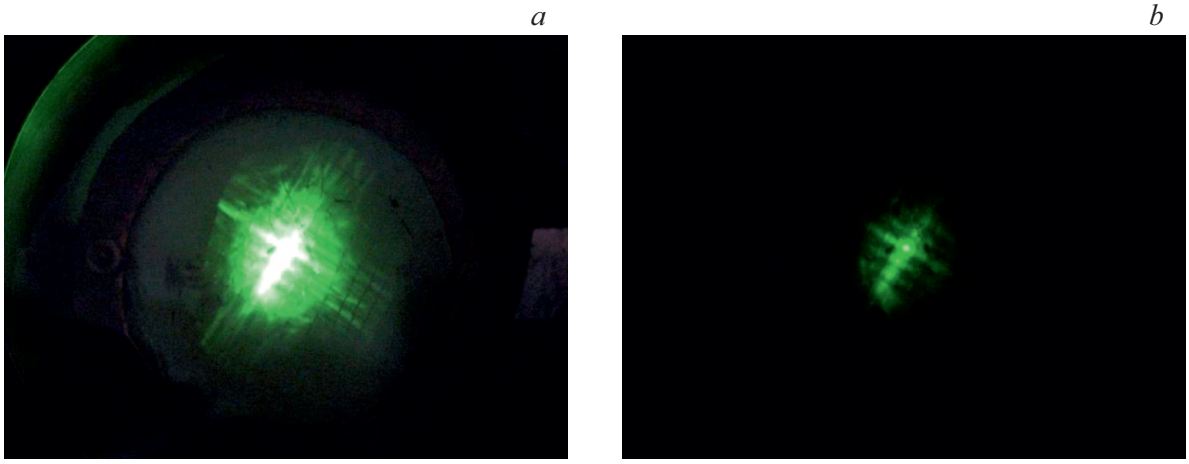

Figure 2. Photographs of flashes of the electron flow at different exposures: a — $\tau = 15$ s; b — $\tau = 2$ s.

preserved [1,11]. In SBN crystals, radiation was completely absent in subsequent heating cycles. Thus, cooling in a vacuum led to depolarization of crystals. Restoration of the operability of SBN crystals was possible only after repeated polarization in an external electric field.

To explain this fact, it is necessary to take into account the small coercive electric field inherent in SBN crystals, $E_c = 2.5$ kV/cm [9]. During heating and cooling, an electric field arises between the polar faces of the crystal which is equaled to the field between the crystal and the target. During heating, the electric field is directed along the polar axis of the crystal and provides additional polarization. When cooled, the electric field is directed against the polarization of the crystal, in which case the crystal is depolarized. We note that the resulting fields can reach values of tens of kV, which significantly exceeds the coercive field.

The polarization of the crystals after cooling was checked by the method of the half-wave voltage [13]. Measurements have shown that the volume polarization of the crystals is preserved and close to the maximum. The explanation for this contradiction is as follows: optical methods measure the polarization in the volume of the crystal, at the same time, in X-ray experiments, the surface charge on the outer face is important. Consequently, the disappearance of the electron beam and X-ray generation is associated with the formation of a domain structure in the region of the upper $c+$ face, while maintaining polarization in the volume of the crystal. The formation of surface domains in the form of pyramids elongated along the axis c was indicated in [14,15].

Multidirectional domains, when heated or cooled, acquire opposite resultant electric charges (Q_{sum}), which should increase as the temperature changes. Obviously, the charges of neighboring domains can be mutually discharged, and, as a result, the total charge and potential become zero. Accordingly, the radiation of crystals with a depolarized surface is absent both during heating and cooling, in accordance with the experiment.

In order to preserve the polarization of the SBN crystals, the samples were cooled at an increased pressure of about $2 \cdot 10^{-1}$ Torr [5], when the compensation of surface charges due to exchange with gas atoms occurred quickly enough, and the total electric field was close to zero. When the temperature of $\approx 10^{\circ}$C was reached, the chamber was pumped back to a pressure of $P \approx 10^{-3}$ Torr, after which the next heating-cooling cycle began.

3. Flashes of electron flow and X-ray radiation

Unusual phenomena with SBN crystals were observed on samples with a depolarized $c+$ face, when filling the working chamber with gas at the end of the heating mode. We studied the sample, which in the previous cycle was cooled in a vacuum of 10^{-3} Torr and had a depolarized surface. When heated in a vacuum, the X-ray radiation and electron beam were completely absent or very weak. When the working chamber was filled with air at a temperature of about 50°C, periodic pulsations of X-ray radiation and electron beam were observed. Radiation pulsations occurred at a pressure of $2 \cdot 10^{-2}$ Torr and continued for about 7 minutes to a pressure of 10^{-1} Torr. A video of the pulsating electron flow is shown in the application file [16]. Figure 2 shows two photographs of the spatial structure of the electron flow taken with different exposures. From the photographs it can be seen that in plan the electron flow has the form of a cross located in the center and oriented along the long axis a of the crystal.

To analyze the data on the electron flow, the resulting video file was modified: the playback time of each frame was increased and a time counter was introduced. Using these tools, the times of occurrence of flashes and their intensity (brightness) were determined. The intensity was determined visually on a scale from 0 to 10. The duration of each flash did not exceed the duration of one frame, i.e.

1/25 s. A graph of the dependence of intensity on time is shown in Fig. 3. Each point corresponds to the time of appearance of the flash and its intensity. As it can be seen from the graph, at the beginning the flashes occur more often, and then more rarely. At the end of the process, the intense flash was observed, corresponding to a complete discharge of the crystal.

The interval between flashes was not constant. Figure 4 shows the intervals between neighboring flashes as a function of time. From the graph it can be seen that the interval increases from the value of 0.2 s to 5 s and more at the end of the process.

Figure 5 shows the data for X-ray radiation. Figure 5, *a* shows the dependence of radiation intensity on time. The acquisition time in each channel was 2 s, i.e. each channel could contain several flashes of radiation. At the beginning of the process, the intensity dependence seems to be continuous due to the small time interval between flashes, however, as the intervals between flashes increase, the dependence also becomes pulsating. From the graph it can be seen that the radiation intensity of the decreases with time.

Figure 5, *b* shows the total pulse height spectrum of X-rays. The spectrum has the form of a wide maximum at energy of ≈ 6 keV and extends to an energy of ≈ 25 keV. We note that the tungsten line L(W) ≈ 8.4 keV, which is characteristic of the heating mode [5], is not observed. The ultimate energy of 25 keV can correspond to the maximum voltage between the crystal and the target in this experiment.

Let us list the main experimental facts.

1. Pulsations have been observed in crystals with a depolarized surface that occurs after cooling in a vacuum.

2. Pulsating electron flow and X-ray radiation was observed at a constant temperature of about 50°C when pressure increased from $2 \cdot 10^{-2}$ to 10^{-1} Torr.

3. In the plane of the crystal, the electron flow had the form of a cross.

4. The flash duration is < 0.04 s. The pulsation period changes from 0.2 s at the beginning and up to 5–10 s at the end at a pressure of $P \approx 0.1$ Torr.

5. The X-ray radiation had a maximum energy of $E \approx 6$ keV; and the bremsstrahlung background extended to 25 keV.

6. In a number of cases, the appearance of surface discharges was observed.

The following interpretation of the observed effect can be proposed.

In the initial state, the upper face of the crystal is in a depolarized multidomain state. Each domain is polarized and has a bound charge Q_{bond} with a density of $+\sigma$ or $-\sigma$ and its compensating surface charge Q_{comp} with a density of $-\sigma$ or $+\sigma$, respectively. The total surface charge and electric potential of each domain are zero. When the chamber is filled with gas, when the pressure reaches $2 \cdot 10^{-2}$ Torr, the domain boundary shifts. This creates a new region with inverse polarization, for example $-\sigma$ with an area of s1. Consider this area as a separate domain

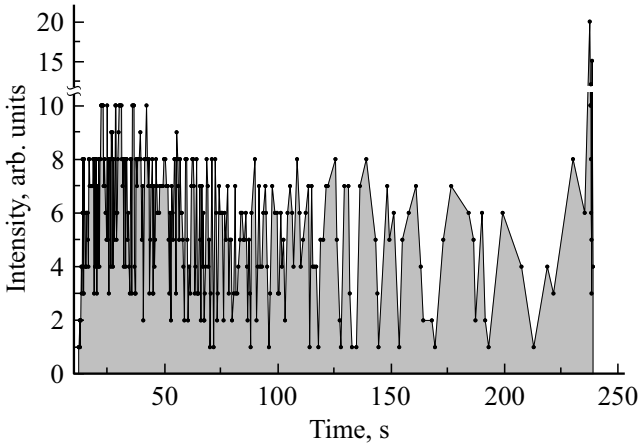

Figure 3. The dependence of the intensity of flashes of electron flow on time.

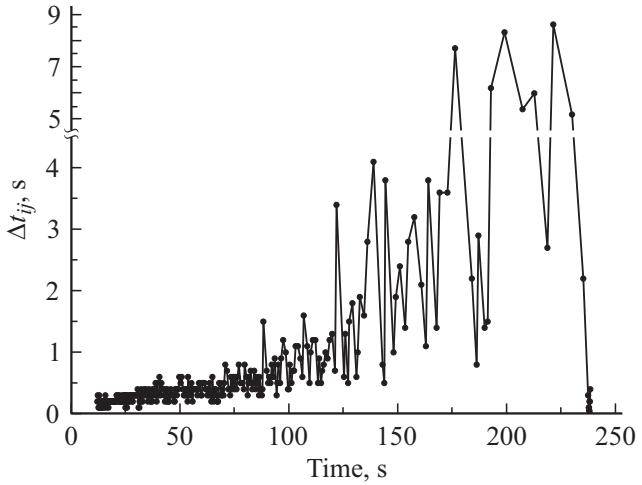

Figure 4. Intervals between neighboring flashes as a function of time.

(see Fig. 6). In its original state, it had a polarization of $+\sigma$ and a surface compensating charge of $-\sigma$ (Fig. 6, *a*, the surface charge is shown by a shaded area). After polarization inversion, the domain has a polarization $-\sigma$. However, the surface compensating charge in this region remains unchanged: $-\sigma$ (Fig. 6, *b*).

Compared to the compensated domains, this domain acquires an excess charge $Q_{\text{P}} = -2\sigma \cdot \text{s1}$. This charge represents a larger magnitude because it corresponds to equilibrium polarization rather than a change in polarization due to a change in temperature. For a crystal SBN-61, the polarization is $P_s = 27.4\,\mu\text{C/cm}^2$, and the surface charge at $\Delta T = 10°\text{C}$ is $\Delta Q = \gamma \cdot \Delta T = 0.85\,\mu\text{C/cm}^2$. If we estimate the voltage that will arise between the domain and the target in our geometry due to the charge Q_{P} according to the formula (1), we get a very large value, about 800 kV.

Obviously, the excess charge Q_{P} will be redistributed over the surface of the crystal. The redistribution of charge can be due to surface conduction or by electro-breakdowns,

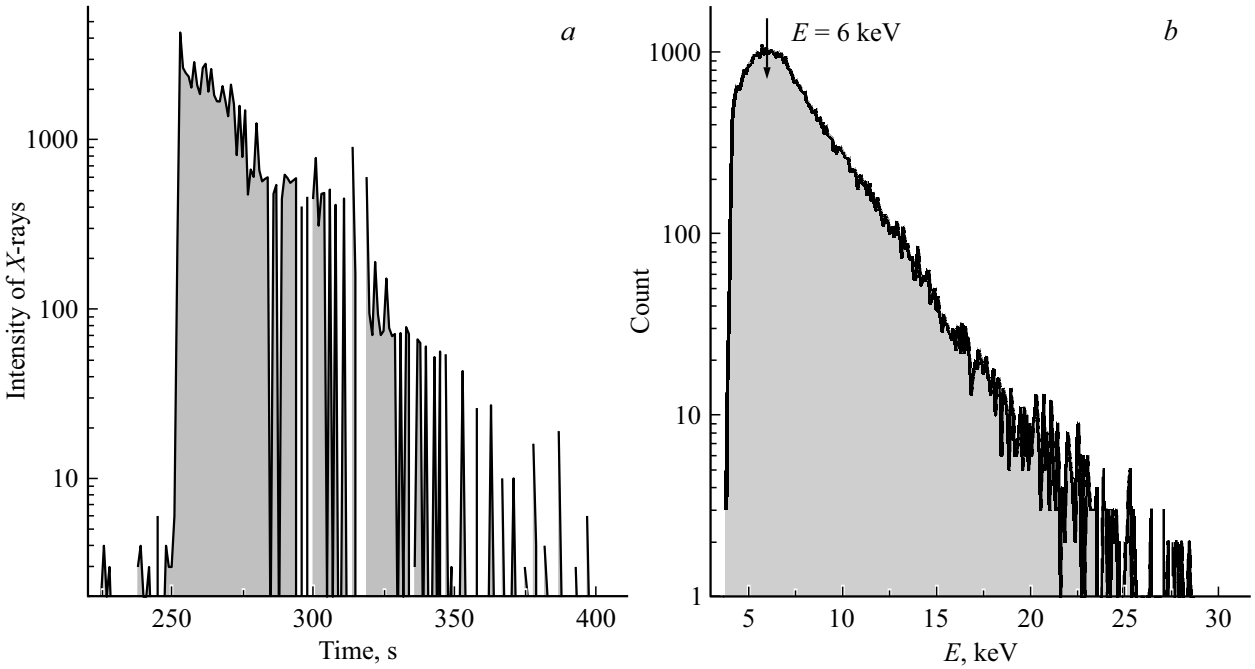

Figure 5. X-ray radiation in pulsating mode: *a* — dependence of the X-ray intensity on time, *b* — pulse height spectrum.

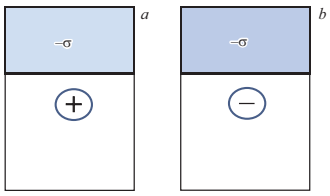

Figure 6. The scheme of formation of the inverse domain: *a* — the original domain with positive polarization $+\sigma$ and surface charge $Q_{\text{comp}} = -\sigma \cdot \text{s1}$, *b* — inverse domain with negative polarization $-\sigma$ and surface charge $Q_{\text{comp}} = -\sigma \cdot \text{s1}$.

since the voltages are very high. If the charge is distributed over an area S, then the excess charge will be equal to $\Delta\sigma = -2\sigma \cdot \text{s1/S}$. In this case, there is an electron flow directed from the crystal to the target. In our experiment, the electron flow was observed from the central region of the crystal, apparently, and the redistribution of charge occurred in the same region.

If the new domain region has a positive polarization $+\sigma$, then the resulting polarization of the surface will be positive. In this case, the electron flow is directed towards the crystal and will not be observed in the experiment.

Thus, our experiment can be explained by the movement of domain boundaries under the influence of increasing gas pressure, provided that additional negatively polarized regions are formed. The movement of domain boundaries in SBN crystals depends on many factors, so this effect was not observed for all samples.

Usually, residual gas and the presence of high voltages lead to the formation of gas discharges. However, in our case, the pressure is small: the mean free paths of electrons for ionization of molecules N_2 is $L_i = 18$ cm at a pressure of $P = 2 \cdot 10^{-2}$ Torr, and $L_i = 3.6$ cm at a pressure of $P = 10^{-1}$ Torr [17], which is significantly greater than the distance between the crystal and the grid, about 0.7 cm. Accordingly, the avalanche ionization of the gas cannot occur. In addition, with a gas discharge, it is difficult to expect the projection of the grid electrode on the phosphor, which was observed in the experiment (Fig. 2). With this in mind, the effect of gas discharges in this experiment seems unlikely.

4. Conclusion

When the crystal SBN-61 is cooled in a vacuum of 10^{-3} Torr, the outer *c*-face is depolarized by the crystal's own electric field while maintaining the volume polarization. As a result, there is neither electron flow, nor generation of X-ray radiation, both in cooling mode and during subsequent heating in the vacuum.

In X-ray generator based on a crystal SBN-61 with a depolarized *c*-face the pulsations of the electron flow and X-ray radiation were detected with an increase in gas pressure in the range of $2 \cdot 10^{-2}$–10^{-1} Torr at a constant temperature of about 50°C.

An explanation of the pulsation mode based on the movement of the of the domain walls at the outer *c*-face of the crystal SBN-61 under the influence of ambient gas pressure is proposed.

This effect can be used to create powerful pulsed electron beams.

Funding

This study was carried out with the support of the Federal Scientific and Technical Program for the Development of Synchrotron and Neutron Research and Research Infrastructure, grant of Ministry of Science and Higher Education of the Russian Federation No. 075-15-2021-1353.

Conflict of interest

The authors declare that they have no conflict of interest.

References

[1] J.D. Brownridge, S. Raboy. J. Appl. Phys. **86**, 640 (1999).
[2] D.J. Gillich, A. Kovanen, Y. Danon. J. Nucl. Mater. **405**, 181 (2010).
[3] K.A. Vokhmyanina, O.O. Ivashchuk, V.Yu. Ionidi, A.A. Kaplii, I.A. Kishchin, A.S. Klyuev, A.S. Kubankin, M.V. Mishunin, R.M. Nazhmudinov, I.S. Nikulin, A.N. Oleinik, A.V. Sotnikov, A.S. Chepurnov, A.V. Shchagin Steklo i keramika **90**, *11*, 24 (2017) (in Russian).
[4] www.amptek.com/coolx.html
[5] V.A. Andrianov, A.L. Erzinkian, L.I. Ivleva, P.A. Lykov. AIP Advances **7**, 115313 (2017); https://doi.org/10.1063/1.5010143.
[6] A.A. Bush. Piroelektricheskiy effekt i ego primeneniya. MIREA, M. (2005). 212 p. (in Russian).
[7] .K. Batra, M.D. Aggarwal. Pyroelectric Materials: Infrared Detectors, Particle Accelerators and Energy Harvesters. SPIE Press, Bellingham, Washington, USA (2013). 546 p. ISBN: 978-0-8194-9331.
[8] W.H. Huang, D. Viehland, R.R. Neurgaonkar. J. Appl. Phys. **76**, 490 (1994).
[9] P.A. Lykov. Vyrashchivanie i issledovanie legirovannykh monokristallov niobata bariya-strontsiya. Diss. kand. nauk. Moscow, (2008). 166 p. (in Russian).
[10] Z. Fullem, Y. Danon. J. Appl. Phys. **106**, 074101 (2009).
[11] V.A. Andrianov, A.A. Bush, A.L. Erzinkyan, K.E. Kamentsev. Poverkhnost': Rentgen., sinkhrotr. i nejtron. issled. **7**, 25 (2017) (in Russian).
[12] L.I. Ivleva. Izv. RAN. Ser. fiz. **73**, *10*, 1417 (2009) (in Russian).
[13] M.Di. Dommenico, S.H. Weple. J. Appl. Phys. **40**, 720 (1969).
[14] N.R. Ivanov, T.R. Volk, L.I. Ivleva, S.P. Chumakova, A.V. Ginzberg. Kristallografiya **47**, 1092 (2002) (in Russian).
[15] V.Ya. Shur, P.S. Zelenovskiy. J. Appl. Phys. **116**, 066802 (2014).
[16] https://disk.yandex.ru/i/OtDscGTR130hbw
[17] Yu.P. Raizer. Fizika gazovogo razryada. Nauka, M. (1992). 536 p. (in Russian).